

Hole redistribution across interfaces in superconducting cuprate superlatticesC. Aruta,^{1,*} G. Ghiringhelli,^{2,3} C. Dallera,⁴ F. Fracassi,³ P. G. Medaglia,⁵ A. Tebano,⁵ N. B. Brookes,⁶ L. Braicovich,³ and G. Balestrino⁵¹*CNR-INFM Coherentia, Dipartimento di Scienze Fisiche, Università di Napoli “Federico II,” Complesso di Monte S. Angelo, Via Cinthia, I-80126 Napoli, Italy*²*CNR-INFM Coherentia, Dipartimento di Fisica, Politecnico di Milano, piazza Leonardo da Vinci 32, I-20133 Milano, Italy*³*CNR-INFM Soft, Dipartimento di Fisica, Politecnico di Milano, piazza Leonardo da Vinci 32, I-20133 Milano, Italy*⁴*CNR-INFM Ultras, Dipartimento di Fisica, Politecnico di Milano, piazza Leonardo da Vinci 32, I-20133 Milano, Italy*⁵*CNR-INFM Coherentia, Dipartimento di Ingegneria Meccanica, Università Tor Vergata, via del Politecnico 1, I-00133 Roma, Italy*⁶*European Synchrotron Radiation Facility, B.P. 220, F-38043 Grenoble cedex, France*

(Received 2 July 2008; revised manuscript received 22 October 2008; published 25 November 2008)

With the aim of disentangling the role of the constituent blocks in the high- T_c cuprate superconductors we have measured x-ray absorption spectra at the Cu L_3 edge on $(\text{Cu}_{1-\delta}\text{C}_\delta)\text{Ba}_2\text{CuO}_x$ (BCO), CaCuO_2 (CCO), and BCO/CCO superconducting superlattices obtained by stacking in a sequence the two blocks. By observing the polarization dependence we could discriminate between the in-plane and out-of-plane hole densities. The results strongly indicate that charge is redistributed across the interfaces from the BCO charge reservoir block to the CCO infinite layer block. In the superconducting samples a relatively high density of out-of-plane holes is still present, whereas when the CCO layer thickness is excessive the holes appear to have preferential in-plane orientation and superconductivity is suppressed.

DOI: [10.1103/PhysRevB.78.205120](https://doi.org/10.1103/PhysRevB.78.205120)

PACS number(s): 74.78.Fk, 74.78.Bz, 74.25.Jb, 73.20.-r

I. INTRODUCTION

Since the discovery of the high-temperature superconductivity (HTS) in $\text{La}_{2-x}\text{Ba}_x\text{CuO}_4$,¹ careful scientific investigations of the electronic structure have been performed to understand the mechanism of superconductivity. The interpretation of the electronic properties of cuprates is made even more difficult by the presence of several structurally inequivalent Cu and O sites. Furthermore, such inequivalent Cu and O ions play a different role as far as superconductivity is concerned. Namely, it is now widely accepted that all HTS cuprates consist of two structural blocks, having different functional properties, stacked along the c axis. The first block, sometimes called “infinite layer” (IL) block, consists of CuO_2 planes separated by a bare cation plane. The second block, which is charge unbalanced by cation substitution or oxygen nonstoichiometry, is thought to act as a charge reservoir (CR) for the IL block. In this simple structural model, charge transfer from the CR block is thought to give rise to superconductivity in the IL block.

On a parallel route, a large effort is being devoted to the study of the interface interaction between different oxides in artificial heterostructures. Namely, interfaces obtained by assembling complex oxides having the perovskite structure show unexpected properties such as high conductivity and magnetism,^{2,3} and even superconductivity.⁴ Those phenomena can be influenced by a variety of parameters such as the number of oxygen vacancies,⁵ the epitaxial strain, the so-called polarization catastrophe from interface-generated dipoles,⁶ and the electronic reconstruction at the interface.⁷ For instance, the observed suppression of superconductivity in manganite/cuprate superlattices (SLs) has been attributed to the strong rearrangement and hybridization of the orbitals at the interface between the two constituent layers.⁸ On the reverse, superconductivity as a consequence of orbital rearrangement has been predicted in $\text{LaNiO}_3/\text{LaMnO}_3$ superlattices.⁹

Standard HTSs are often considered as “natural superlattices” made of CR and IL blocks. In this sense some sort of “interaction at the interfaces” can be foreseen even for these compounds. However, in this case, such an effect cannot be easily singled out as the “interface interaction” cannot be switched on by separating the constituent blocks.

Here we propose a different approach to the investigation of the electronic properties of HTS cuprates. Namely, we have disassembled the superconductor in the constituent blocks and measured separately the CR and the IL blocks, which, in our case, consist of the $(\text{Cu}_{1-\delta}\text{C}_\delta)\text{Ba}_2\text{CuO}_x$ (BCO) and the CaCuO_2 (CCO) compounds, respectively. Moreover, artificial superconducting superlattices, obtained by stacking in a sequence the two blocks, have been also measured. The schematic representation of the atomic stacking sequence and the arrangement of the BCO/CCO superlattices is reported in Fig. 1(a). On such samples we have performed polarization-dependent x-ray absorption spectroscopy (XAS) measurements at the Cu L_3 absorption edge in order to investigate the hole doping. Electron spectroscopic techniques have been intensively used in studying the electronic states near the Fermi level in these rather complex materials.¹⁰ In particular, polarized XAS measurements demonstrated to be an important tool to study the hole symmetry in the high- T_c cuprates.

II. EXPERIMENTAL DETAILS

High oxygen pressure pulsed laser deposition technique has been employed to grow the single constituent blocks (BCO and CCO) and the $\text{BCO}_N/\text{CCO}_M$ artificial superlattices on (001) SrTiO_3 substrate. Details of the growth process are reported elsewhere.¹¹ In the superlattices we kept the number of the charge reservoir BCO blocks fixed while varying the number M of CCO blocks between 2 and 12. A single unit cell of the BCO compound comprises two Ba planes so

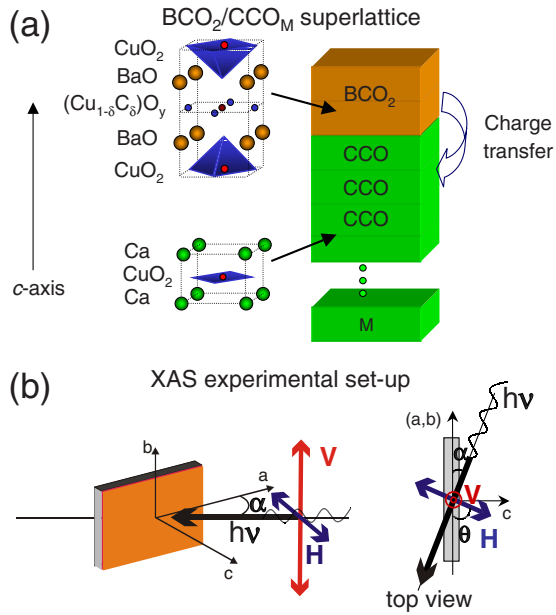


FIG. 1. (Color online) (a) Atomic stacking sequence and arrangement of atoms of the BCO/CCO superlattices with a schematic representation of the hole transfer from the charge reservoir BCO block into the infinite layer CCO block. (b) Schematic of the experimental setup used to obtain the polarized XAS data in horizontal (H) and vertical (V) polarizations. To get the hole symmetry dependence, the film plane is tilted of an α angle with respect to the photon beam propagation direction.

that we refer to it as $N=2$ ($2 \times M$ superlattices). Because of the high oxygen background pressure (about 10^{-1} mbar) during film deposition, the direct calibration of the deposition rate by *in situ* high-energy electron diffraction was not possible. Calibration of the growth rates, precise at the level of a single unit cell, was obtained *a posteriori* by reflectivity and x-ray diffraction (XRD) measurements.¹² Structural properties of films were measured by XRD at the Cu $K\alpha$ wavelength in the Bragg-Brentano configuration using a laboratory x-ray source. Electrical transport properties were investigated as a function of temperature by the standard four-probe technique.

XAS measurements at the Cu L_3 edge were performed at the ID08 beamline of ESRF in Grenoble, detecting the sample drain current. The beamline source was an AppleII undulator delivering almost 100% polarized radiation and equipped with a Dragon-type monochromator. The energy resolution was 160 meV. Measurements were carried out by varying the x-ray beam incidence angle and the linear polarization direction from horizontal (H) to vertical (V). A linear background was subtracted from the XAS spectra and the intensity values at different angles were corrected by a scale factor in order to account for the different geometries. Because in V polarization the electric \mathbf{E} vector was always parallel to the sample surface (ab plane), whatever the angle of incidence, the scale factors were experimentally obtained in V polarization from the ratio among the main edge intensities at different angles. A schematic representation of the experimental setup of the XAS measurements is reported in Fig. 1(b).

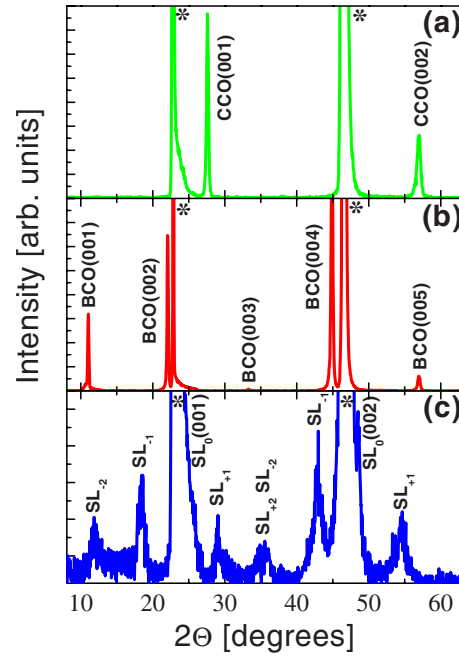


FIG. 2. (Color online) $\Theta-2\Theta$ XRD spectra of the (a) CCO, (b) BCO, and (c) 2×2 superlattice on SrTiO_3 substrate. The asterisks indicate the peaks from the substrate. Peaks indexed by SL refer to the satellite peaks from the superlattice structure.

III. RESULTS

A. Structural and transport properties

BCO films having the infinite layer structure are difficult to grow because of the strong tendency of this compound to incorporate extra oxygen ions in the Ba planes. This feature was proved by extended x-ray absorption fine-structure (EXAFS) measurements, which showed the presence of apical oxygen atoms in the Ba block.¹³ XRD has shown that at relatively high oxygen background pressure ($\geq 10^{-1}$ mbar), oxygen ions tend to fill the Ba planes, while each other CuO_2 plane is oxygen depleted. Consequently, the perpendicular lattice parameter is doubled ($c=8.16$ Å) if compared to the pure infinite layer phase [compare diffraction spectra (a) and (b) in Fig. 2]. Furthermore, even if in our case no CO_2 is deliberately added in the growth atmosphere, it is known that the oxygen-depleted CuO_2 planes have a strong tendency to incorporate residual carbon.¹⁴ As a result of the overall oxygen excess, BCO films are slightly metallic with a resistivity upturn below 60 K [Fig. 3, curve (b)]. However, no evidence of superconductivity was found down to 4 K in our BCO films. On the contrary, it has been reported that when CO_2 partial pressure is deliberately added in the background atmosphere, CO_3 groups can fill Cu vacancies in the CuO_{2-y} planes (see Fig. 1 of Ref. 14) so that the BCO compound itself becomes superconductor with an onset temperature for the transition as high as 40 K.^{14,15} In conclusion, we can argue that, most likely, the formula unit of our BCO films can be written as $(\text{Cu}_{1-\delta}\text{C}_\delta)\text{Ba}_2\text{CuO}_x$ with δ smaller than that found in superconducting samples.

By stacking in a sequence a single unit cell of the BCO compound and two unit cells of CCO, the so-called 2×2

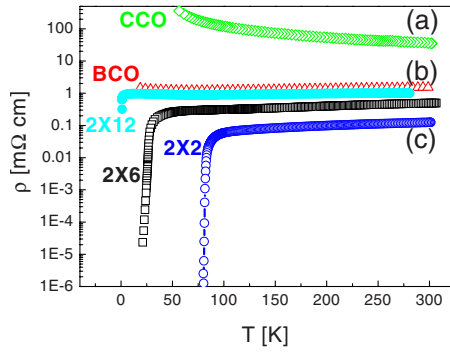


FIG. 3. (Color online) Resistivity as a function of temperature for the (a) CCO, (b) BCO, and (c) 2×2 superlattice. The resistivity behaviors of the 2×6 and 2×12 superlattices are also reported.

superconducting superlattice [Fig. 3, curve (c)] with the highest critical temperature $T_c = 80$ K is obtained [the XRD spectrum is reported in Fig. 2(c)]. By increasing the number of CuO_2 planes in the IL block, T_c goes smoothly to zero and for the 2×12 superlattice the critical temperature (zero resistance point) is about 1 K. An even higher number of CuO_2 planes in the IL block give rise to an insulating behavior.¹¹

B. XAS measurements

XAS spectra at Cu L_3 edge for different incidence angles and different polarizations are reported for (a) BCO, (b) CCO, and (c) the 2×2 superlattice in Fig. 4. The x-ray beam was set at different incidence angles with respect to the sample surface, namely, $\alpha = 10^\circ$, 15° , and 30° . In these conditions, with H polarization, the angle between the electric-

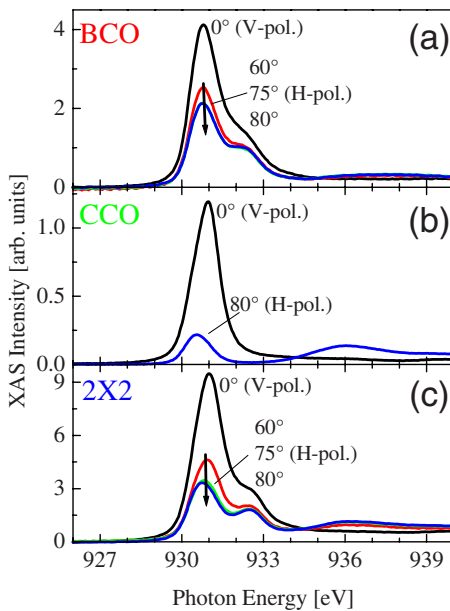


FIG. 4. (Color online) Polarized XAS measurements of the (a) CCO, (b) BCO, and (c) 2×2 superlattice. Measurements were taken at V and H polarization of the x rays and with different incidence angles. XAS data are labeled by θ angles between the electric-field vector and the sample surface, as sketched in Fig. 1(b).

field vector \mathbf{E} of the incident beam and the sample surface was $\theta = 80^\circ$, 75° , and 60° , respectively. On the other hand, with V polarization, \mathbf{E} lies always in the ab plane, namely, $\theta = 0^\circ$. For all XAS spectra of Fig. 4, the main peak at about 931.0 eV corresponds to the $3d^9$ initial-state configuration ($3d^9 \rightarrow 2p^5 3d^{10}$ transition with a Cu $2p_{3/2}$ electron being promoted to the Cu $3d$ orbital when a photon is absorbed).¹⁶ A shoulder, 1.4 eV above the main peak, is evident in Fig. 4(a) (BCO sample) and Fig. 4(c) (2×2 superlattice). Such a shoulder is usually associated with the $3d^{10}\underline{L}$ final-state configuration, where \underline{L} denotes a $2p$ hole at the oxygen sites surrounding the Cu absorbing atom in the CuO_2 plane. In other words, this peak is characteristic of the absorption of one photon at a site hosting a double hole, i.e., a Zhang-Rice singlet (ZRS). We denote this transition as $3d^9 \underline{L}_{\text{ZRS}} \rightarrow 2p^5 3d^{10} \underline{L}$, where the final state is localized at the Cu site hosting the ZRS. Aside from these well-known peaks we have to consider a third type of transition, involving more delocalized states. We denote as $3d^9 \underline{L} \rightarrow 2p^5 3d^{10} S$ a transition where the $2p$ core hole in the final state is well screened by electrons not belonging to the absorbing Cu and neighboring oxygen atoms. The energy of this transition is usually very close to that of $3d^9 \rightarrow 2p^5 3d^{10}$, i.e., 931.0 eV.^{17,18} As a consequence, the main L_3 peak has two components: one given by the undoped sites ($3d^{10}$ final state) and one by the well-screened final states ($3d^{10}S$).

Due to the local noncubic symmetry at the copper ions both in BCO and CCO, among the e_g states the $x^2 - y^2$ orbital usually hosts the hole for the undoped sites, and also the ZRS has $x^2 - y^2$ symmetry. This preferential occupation gives rise to a strong linear dichroism of the XAS signal: when the electric vector \mathbf{E} is in the ab plane the transition to the $x^2 - y^2$ orbital is possible; when \mathbf{E} is along the c axis it is forbidden.

As with XAS we are probing many layers, in the naive hypothesis that the two constituent blocks do not modify their electronic structure when stack in a superlattice, one would expect that the spectra of the 2×2 superlattice could be obtained as the average of the BCO and the CCO individual spectra. In Fig. 5(a) we compare the real spectrum of the 2×2 sample with the one given by the average of BCO and CCO for the V polarization ($\mathbf{E} \parallel ab$). In order to perform a qualitative comparison of the spectra we have normalized to unity the intensity of the main peak (931.0 eV) measured with $\mathbf{E} \parallel ab$ (spectra at 0° in Fig. 4). The spectrum from the superlattice is clearly different from the one given by the average of individual block spectra. The same procedure was applied for the XAS spectra taken with H polarization ($\mathbf{E} \parallel c$). The discrepancy between the experimental data and the calculation performed by averaging the BCO and CCO spectra is even more pronounced. This is a strong evidence of the deep changes intervening in the electronic structure of BCO and CCO when they are strongly coupled together in a superlattice: charges are exchanged across the interface and a new original material is born.

With the purpose of making a more quantitative assessment of the charge transfer across the interface and of the reorganization of the holes in the superlattices we have computed, from the experimental spectra, the “doping hole density,” i.e., the ratio of the spectral weight at 932.4 eV to the

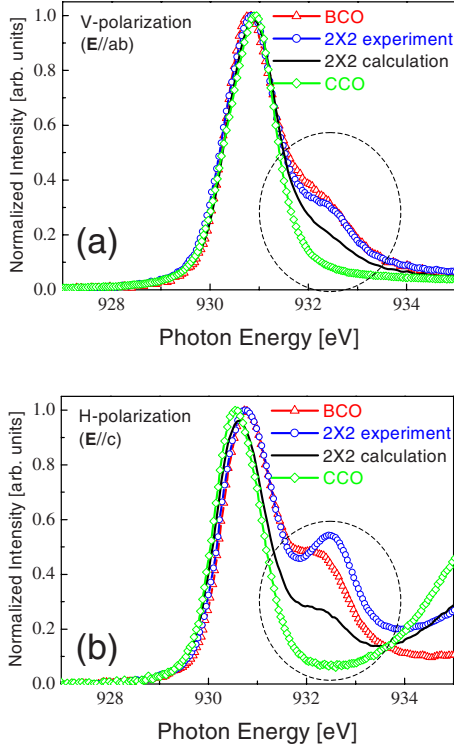


FIG. 5. (Color online) Normalized to unity XAS measurements of the BCO (empty triangles), the 2×2 superlattice (empty circles), and the CCO (empty diamonds). The calculated XAS spectra in case of noninteracting blocks are also reported (continuous line). The dashed circle encompasses the $3d^9L$ peak region. The measurements are taken with the electric-field vector in the (a) ab plane and (b) parallel to the c axis.

total intensity: $n_h = I_{932.4} / [I_{931.0} + I_{932.4}]$. This number can be calculated both for V and H polarizations, getting thus an estimate of the ZRS density for $\mathbf{E} \parallel ab$ and of the out-of-plane “localized” double-hole occupancy for $\mathbf{E} \parallel c$.¹⁹ $I_{931.0}$ and $I_{932.4}$ represent the integrated intensity of the Gaussian fit of the two partially overlapping peaks clearly discernible across the Cu L_3 region. In Fig. 6 we report the n_h values for the pure constituents and for three $N \times M$ superlattices, namely, 2×2 , 2×6 , and 2×12 ; both the in-plane and out-of-plane results are shown. The abscissa is given by the fraction of CCO, $f = \frac{M}{M+N}$; $f=0$ and $f=1$ correspond to the pure BCO and CCO compounds, respectively. The data for $\mathbf{E} \parallel c$ were obtained by extrapolating to 90° the intensities measured at different angles with H polarization: $I(\theta) = I(0^\circ)\cos^2(\theta) + I(90^\circ)\sin^2(\theta)$.²⁰ In order to highlight the difference between the experimental results and what would result in case of noninteracting blocks, in the same figure we show the curves computed according to the model, namely,

$$n_h = \frac{fB_{\text{CCO}} + (1-f)B_{\text{BCO}}}{f(A_{\text{CCO}} + B_{\text{CCO}}) + (1-f)(A_{\text{BCO}} + B_{\text{BCO}})}$$

$$= \frac{B_{\text{CCO}=0}}{fA_{\text{CCO}} + (1-f)(A_{\text{BCO}} + B_{\text{BCO}})},$$

where the fraction f has been supposed to vary continuously

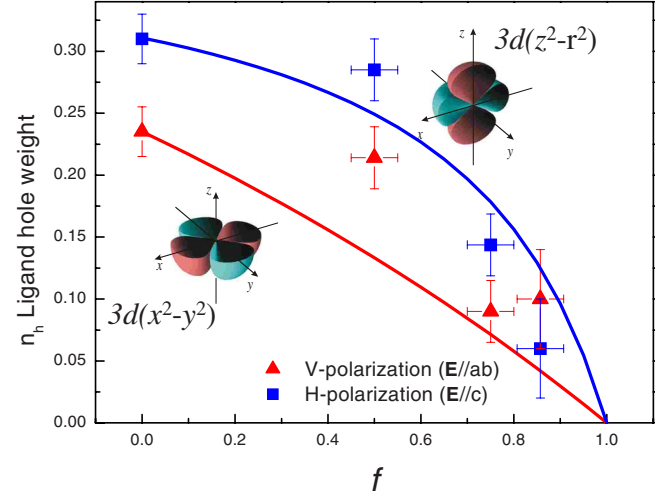


FIG. 6. (Color online) Doping holes density calculated by the XAS measurements as described in the text, with the electric-field vector in the ab plane (full triangles) and parallel to the c axis (full squares). Data are reported as a function of the CCO fraction f . The continuous lines are the calculated behaviors in case of noninteracting constituent blocks. The in-plane and out-of plane Cu^{2+} orbitals are also reported as insets.

from 0 to 1 and A_{CCO} (A_{BCO}) and B_{CCO} (B_{BCO}) are the integrated intensities of the peaks at 931.0 and 932.4 eV, respectively, obtained from the experimental spectra of the pure CCO block (BCO block). As in CCO the intensity at 932.4 eV is zero, $B_{\text{CCO}}=0$. We can see at a glance that the 2×2 case deviates for the “noninteracting-blocks” (NIB) model both for holes in plane and out of plane. The discrepancy becomes less evident for the 2×6 and 2×12 superlattices.

IV. DISCUSSION

In the hole-doped superconducting cuprates the carrier distribution over the unit cell and the charge-transfer mechanism are still under debate. The interplay among the Cu–O bond lengths, the cation sizes, and the Cu valence may affect the hole-doping level of the CuO_2 plane.²¹ Structural and chemical properties are closely bound up with the local-orbital character of the carriers in hole-doped cuprates. Ohta *et al.*²² proposed that the different position of the apical oxygen was directly related to T_c . Feiner *et al.*²³ proposed that the p_z orbital of the apical oxygen hybridizing with the $d_{3z^2-r^2}$ orbital of Cu and the $p_{x,y}$ orbitals of the in-plane oxygen affects the next-nearest-neighbor hopping in the CuO_2 plane. However, the important question of the symmetry of the itinerant doping holes responsible for superconductivity is still an outstanding problem. Our experimental results reconcile the different findings by revealing the peculiar holes symmetry contribution of each constituent block and the importance of the charge transfer in determining the resulting holes symmetry in the superconducting sample. The comparison between experimental results and NIB model presented in Figs. 5 and 6 leads to a relatively straightforward

general interpretation that we anticipate before entering the technical details of the spectral assignments. In the superlattices doping holes are distributed over the two constituent blocks and are not confined to BCO, which “naturally” grows as overdoped. This redistribution brings into the CuO_2 planes originally belonging to CCO an amount of hole doping compatible with superconductivity if the appropriate stacking ratio is chosen. The BCO block can act as a charge reservoir (very similarly to normal HTS) thanks to the three-dimensional (3D) distribution of Cu–O bonds guaranteed by the O sites located in the Ba planes, thus, allowing the necessary bridge among the superconducting CuO_2 planes. When the BCO blocks are separated by an increasing number of CCO blocks, T_c gradually decreases until a too thick CCO buffer is no longer sufficiently doped to set up superconductivity. In this case, although the interblock doping mechanism still works, the sample overall is not superconducting: the potentially superconducting CuO_2 planes in the IL layer, because of the lack of bridging apical oxygen ions, are isolated from one another. It has also been reported that the strain effect is an additional source of degradation of the superconducting properties in cuprate superlattices.²⁴ However, we can rule out that the T_c variation is influenced by the strain in the investigated samples because they are all completely strained so that interatomic distances do not vary from sample to sample.

As mentioned above the interpretation follows quite directly in consideration of the peak assignments introduced in Sec. III. First we look at the spectra of pure CCO and BCO. For CCO we measure typical spectra of undoped compounds: one single peak at 931.0 eV showing strong polarization dependence. Cu sites are (almost) all in $3d^9$ configuration, with holes occupying the x^2-y^2 orbital. The relatively weak peak measured with $\mathbf{E}\parallel c$ could be ascribed to O defects: some Cu sites loose the anisotropic behavior, giving origin to a peak at 930.6 eV equally intense with $\mathbf{E}\parallel c$ and $\mathbf{E}\parallel ab$. We notice that the intensity at 931.0 eV goes practically to zero for $\mathbf{E}\parallel c$. On the contrary the BCO spectra are composed of two peaks: at 932.4 eV (double-hole occupancy on the site, unscreened XAS final state indicated as $3d^{10}\bar{L}$) and 931.0 eV for the undoped ($3d^9$) and doped (nonlocally screened XAS final states $3d^{10}S$) sites. The anisotropy is reduced because of the great amount of O ions embedded in the Ba plane, acting as apical oxygen sites for Cu. The two peaks show similar polarization dependence, indicating that localized $3d^9\bar{L}$ sites can have $3z^2-r^2$ or x^2-y^2 symmetry. When intimately coupled in the 2×2 superlattice, CCO and BCO redistribute holes among them, while mainly keeping the “original” hole symmetry. In fact n_h gets only slightly reduced with respect to the pure BCO case and by roughly the same fraction for $\mathbf{E}\parallel ab$ and $\mathbf{E}\parallel c$. As n_h measures only the density of *localized* $3d^9\bar{L}$ sites (renormalized to the total number of holes), the high value of n_h can be due to the localization within the CuO_2 planes of CCO of part of the holes originally delocalized in BCO. In other terms some spectral weight is transferred in the 2×2 superlattice from the 931.0-eV to the 932.4-eV peak. This is the signature of a transfer of hole doping from BCO to CCO. This obviously is

a simplified picture because in the 2×2 SL it is not possible to assign any given CuO_2 plane to CCO or BCO only as in half of the cases CuO planes have Ca layer on one side and Ba layers on the other. The results at the Cu L edge are in agreement with previous XAS measurements at the oxygen K edge performed at the Advanced Light Source in Berkley (USA) on similar samples grown by the same procedure.²⁵ Indeed, in Fig. 2 of Ref. 25 it can be observed as the effect of the charge transfer from the BCO to the CCO blocks is to enhance the doping-related peak at about 528 eV in the O K -edge spectra of the 2×2 sample.

For the 2×6 and 2×12 superlattices this picture is roughly confirmed, although the data analysis is more difficult. From Fig. 6 it seems that when thicker CCO layers separate the BCO charge reservoir layers the hole redistribution takes place preferentially in plane (the experimental values are systematically higher than the NIB model predictions for $\mathbf{E}\parallel ab$), whereas the out-of-plane $3d^9\bar{L}$ sites tend to decrease very rapidly going to higher values of f . This latter fact might indicate a reduced coupling between doped CuO_2 layers, which eventually reduces T_c or even forbids superconductivity at all.

Doping holes with out-of-plane O $2p_z$ and Cu $3d_{3z^2-r^2}$ orbital characters were already reported in several articles, for example, in the case of thallium cuprates by Srivastava *et al.*²⁶ or $\text{YBa}_2\text{Cu}_3\text{O}_x$ by Nücker *et al.*²⁷ However, Chen *et al.*²⁸ found a significant amount of O $2p_z$ holes, likely associated with apical oxygen, and few Cu $3d_{3z^2-r^2}$ holes in $\text{La}_{2-x}\text{Sr}_x\text{CuO}_4$, which increase with the doping by chemical substitution. Here we are adding to the literature general picture further information on the role of the interface between the CR and IL blocks, which is fundamental in establishing the redistribution of a significant number of doping holes from nonlocalized states in the CR to ZRS states in the conducting CuO_2 planes. A similar effect of charge transfer from the CuO chains into the CuO_2 planes was recently observed in the XAS spectra of $\text{NdBa}_2\text{Cu}_3\text{O}_{7-\delta}$ under the application of an external electric field.²⁹

In order to additionally understand the role of the interface between the CR and the IL blocks, further information on the effective thickness for the charge transfer of the CR block can be useful. Therefore, XAS measurements as a function of the CR block thickness are desirable.

V. CONCLUSION

The currently accepted “structural model” on the origin of superconductivity from mutual interaction at the interface via a charge (holes) transfer from the CR to the IL block is difficult to probe experimentally. Indeed, it is impossible to switch on and off the interface interaction in standard compounds. From the comparison between the experimental data referring to the constituent layers and the superlattice we were able to single out the effect of the mutual interface interaction. Namely, we obtained the evidence of strong redistribution of holes across the interface with the doping of CuO_2 planes of the IL block from the out-of-plane orbitals of the CR block. The presence of apical oxygen ions at the

interface seems to be a relevant structural feature for charge redistribution. Suppression of superconductivity for thicker IL layers is likely connected with lack of apical oxygen ions over several CuO₂ atomic planes.

ACKNOWLEDGMENT

We thank Elettronica Masel s.r.l. for a partial financial support.

*aruta@na.infn.it

- ¹J. G. Bednorz and K. A. Müller, *Z. Phys. B: Condens. Matter* **64**, 189 (1986).
- ²A. Brinkman, M. Huijben, M. van Zalk, J. Huijben, U. Zeitler, J. C. Maan, W. G. van der Wiel, G. Rijnders, D. H. A. Blank, and H. Hilgenkamp, *Nature Mater.* **6**, 493 (2007).
- ³A. Ohtomo and H. Y. Hwang, *Nature (London)* **427**, 423 (2004).
- ⁴N. Reyren, S. Thiel, A. D. Caviglia, L. Fitting Kourkoutis, G. Hammerl, C. Richter, C. W. Schneider, T. Kopp, A.-S. Retschi, D. Jaccard, M. Gabay, D. A. Müller, J.-M. Triscone, and J. Mannhart, *Science* **317**, 1196 (2007).
- ⁵A. Kalabukhov, R. Gunnarsson, J. Borjesson, E. Olsson, T. Claesson, and D. Winkler, *Phys. Rev. B* **75**, 121404(R) (2007).
- ⁶J. N. Eckstein, *Nature Mater.* **6**, 473 (2007).
- ⁷L. Brey, *Phys. Rev. B* **75**, 104423 (2007).
- ⁸J. Chakhalian, J. W. Freeland, H.-U. Habermeier, G. Cristiani, G. Khaliullin, M. van Veenendaal, and B. Keimer, *Science* **318**, 1114 (2007).
- ⁹J. Chaloupka and G. Khaliullin, *Phys. Rev. Lett.* **100**, 016404 (2008).
- ¹⁰See, e.g., J. Fink, N. Ncker, E. Pellegrin, H. Romberg, M. Alexander, and M. Knupfer, *J. Electron Spectrosc. Relat. Phenom.* **66**, 395 (1994).
- ¹¹G. Balestrino, S. Lavanga, P. G. Medaglia, S. Martellucci, A. Paoletti, G. Pasquini, G. Petrocelli, A. Tebano, A. A. Varlamov, L. Maritato, and M. Salvato, *Phys. Rev. B* **62**, 9835 (2000).
- ¹²C. Aruta, M. Angeloni, G. Balestrino, P. G. Medaglia, P. Orgiani, and A. Tebano, *J. Appl. Phys.* **94**, 6991 (2003); C. Aruta, F. Ricci, G. Balestrino, S. Lavanga, P. G. Medaglia, P. Orgiani, A. Tebano, and J. Zegenhagen, *Phys. Rev. B* **65**, 195408 (2002).
- ¹³S. Colonna, F. Arciprete, A. Balzarotti, G. Balestrino, P. G. Medaglia, and G. Petrocelli, *Physica C* **334**, 64 (2000).
- ¹⁴K. Kikunaga, K. Takeshita, T. Yamamoto, T. Okuda, Y. Tanaka, N. Kikuchi, K. Tokiwa, T. Watanabe, A. Sunderesan, and N. Terada, *Supercond. Sci. Technol.* **20**, S455 (2007).
- ¹⁵S. Singh, Y. Tanaka, and A. Sunderesan, *Physica C* **466**, 111 (2007).
- ¹⁶D. D. Sarma, O. Strelbel, C. T. Simmons, U. Neukirch, G. Kaindl, R. Hoppe, and H. P. Müller, *Phys. Rev. B* **37**, 9784 (1988).
- ¹⁷T. Mizokawa, T. Konishi, A. Fujimori, Z. Hiroi, M. Takano, and Y. Takeda, *J. Electron Spectrosc. Relat. Phenom.* **92**, 97 (1998).
- ¹⁸G. Ghiringhelli, N. B. Brookes, C. Dallera, A. Tagliaferri, and L. Braicovich, *Phys. Rev. B* **76**, 085116 (2007).
- ¹⁹N. Merrien, F. Studer, G. Poullain, C. Michel, A. M. Flank, P. Lagarde, and A. Fontaine, *J. Solid State Chem.* **105**, 112 (1993).
- ²⁰N. L. Saini, D. S.-L. Law, P. Pudney, P. Srivastava, A. Menovsky, J. J. M. Franse, H. Ohkubo, M. Akinaga, F. Studer, and K. B. Garg, *Physica C* **251**, 7 (1995).
- ²¹Maarit Karppinen and Hisao Yamauchi, *Mater. Sci. Eng., R.* **26**, 51 (1999).
- ²²Y. Ohta, T. Tohyama, and S. Maekawa, *Phys. Rev. B* **43**, 2968 (1991).
- ²³R. Raimondi, J. H. Jefferson, and L. F. Feiner, *Phys. Rev. B* **53**, 8774 (1996).
- ²⁴M. Varela, Z. Sefrioui, D. Arias, M. A. Navacerrada, M. Luca, M. A. López de la Torre, C. León, G. D. Loos, F. Sánchez-Quesada, and J. Santamaría, *Phys. Rev. Lett.* **83**, 3936 (1999).
- ²⁵B. Freelon, A. Augustsson, J.-H. Guo, P. G. Medaglia, A. Tebano, and G. Balestrino, *Phys. Rev. Lett.* **96**, 017003 (2006).
- ²⁶P. Srivastava, B. R. Sekhar, C. Gasser, F. Studer, K. B. Garg, C. T. Chen, and M. Pompa, *J. Phys.: Condens. Matter* **10**, 3417 (1998).
- ²⁷N. Nücker, E. Pellegrin, P. Schweiss, J. Fink, S. L. Molodtsov, C. T. Simmons, G. Kaindl, W. Frentrop, A. Erb, and G. Müller-Vogt, *Phys. Rev. B* **51**, 8529 (1995).
- ²⁸C. T. Chen, L. H. Tjeng, J. Kwo, H. L. Kao, P. Rudolf, F. Sette, and R. M. Fleming, *Phys. Rev. Lett.* **68**, 2543 (1992).
- ²⁹M. Salluzzo, G. Ghiringhelli, J. C. Cezar, N. B. Brookes, G. M. De Luca, F. Fracassi, and R. Vaglio, *Phys. Rev. Lett.* **100**, 056810 (2008).